Radiation Exposure and Protection

21

Judy R. James, T. Michael Martin, and Yun Liang

Introduction

The importance of radiation protection in the interventional radiology department cannot be underestimated. The process of ensuring radiation protection is managed by a team that comprises physicists, radiologists, radiation safety officers, departmental administrators, as well as radiologic technologists. Any radiation exposure can lead to some amount of risk to all the individuals involved, including not only patients but also physicians, technologists, nurses, and other staff participating in the procedure. While patients and staff are exposed to fundamentally different types of radiation (i.e., direct vs. scattered), the reduction of exposure to one group is equally manifested in the other group. At the most basic level, exposure can be minimized by adequate training and proper handling of equipment and X-ray sources. The primary objective of radiation protection is to balance the risks and benefits from all procedures that involve radiation, that is, to maintain adequate image quality while minimizing exposure to all involved. To control this aspect, several regulations are put in place by national organizations to minimize consequences due to improper use of the X-ray producing devices or sources.

In this chapter, the numerous risks related to radiation exposure from fluoroscopy and computed tomography (CT) procedures for spinal interventions are outlined, with special attention given to mitigation of these risks. This chapter will cover the different regulations that govern radiation protection in hospitals. Recommendations for occupational radiation protection techniques and patient safety guidelines are also covered. The risks and benefits of using lead shielding, proper and timely calibration and checks on equipment, and other practical factors are also outlined.

Fluoroscopy-Guided Spinal Procedures and Patient Doses

Spinal interventional procedures are gaining momentum in the diagnosis and treatment of various spinal pathologies of benign or malignant origin [1]. Biplane fluoroscopy and rotational flat panel with cone beam CT (CBCT) capabilities are some of the emerging modalities for enhanced image guidance during difficult spinal procedures.

J. R. James (✉)
Department of Radiology, Loyola University Medical Center, Maywood, IL, USA
e-mail: judy.james@lumc.edu

T. M. Martin
Health Physics and Radiation Safety, Department of Radiology and Imaging Sciences, Indiana University, Indianapolis, IN, USA

Y. Liang
Department of Radiology and Imaging Sciences, Indiana University, Indianapolis, IN, USA

M. Khan et al. (eds.), *Image Guided Interventions of the Spine*,
https://doi.org/10.1007/978-3-030-80079-6_21

Fluoroscopic systems are typically operated in three operational modes: fluoroscopic, radiographic (acquisition), and serial image sequences such as digital subtraction angiography (DSA) and cineradiography (CINE). The radiation dose that is delivered in interventional fluoroscopy procedures is typically highly variable and dependent upon multiple factors [2, 3]. These factors include diagnostic vs. therapeutic purposes, the complexity of patient anatomy involved, patient size, experience of the fluoroscopist, and hardware/software featured in the fluoroscopy instrumentation. These combined factors determine the length of the procedure and the cumulative dose to the patient, operators, and staff. Due to variation among different imaging systems, differences in patient anatomy and procedure complexity, and techniques used by differing physicians, standardization of fluoroscopy protocols is difficult at best.

Imaging Procedures

Physicians use fluoroscopy that involves a series of repeated short-pulse X-rays to generate dynamic images, to visualize and monitor patient anatomy in real time while performing needle and catheter insertions. The pulse repetition for a fluoroscopy exam is programmed at a frame rate typically ranging from 3 fps (frame per second) to 30 fps. Fluoroscopy is used almost exclusively for positioning of the tube relative to patient, needles, catheters, or therapeutic agents; therefore, diagnostic-level image quality is not required. A single frame fluoroscopic exposure is generally associated with very low tube current and much lower radiation exposure when compared with conventional radiographic images. However, since many frames are acquired (ranging from 180 to 1800 frames per minute of fluoroscopy time), the total radiation dose can be substantial and much higher than the doses associated with simple radiographic examinations. During the procedure, physicians often need to capture and record images for diagnostic evaluation; therefore, additional radiation exposure is delivered for select image acquisitions. For these acquisitions, the delivered radiation dose is comparable to conventional single projection radiographic imaging. When sophisticated acquisitions such as DSA and CINE are required by the fluoroscopist, considerable patient doses are expected.

Patient Dose Estimation

For fluoroscopically guided spinal procedures, a primary concern is skin entrance surface dose, as the X-ray beam may be directed to the same area for a prolonged time period. In these scenarios, deterministic radiation effects (such as erythema, epilation, etc.) become a real possibility. However, estimating skin entrance surface dose is far from straightforward. Direct measurements of skin dose is theoretically possible by using radiation sensors, such as thermoluminescence dosimeters (TLDs) or metal oxide semiconductor field effect transistor (MOSFET) detectors or radiosensitive film (Gafchromic™) placed on the skin surface [4–8]. However, this approach is largely impractical in the clinical setting due to interference with clinical techniques and the lack of real-time data; therefore, these measurements are generally related to phantom-based studies. In an effort to apply practical real-time estimations and to reduce skin dose effects, several regulations and equipment standards have been introduced.

In 2000, the International Electro-technical Commission (IEC) introduced the concept of "reference dose" [9], which is simply the air kerma (AK, measured in Gy) at a fixed Interventional Reference Point (IRP); this is commonly abbreviated as AK_R. Additionally, since 2006, the US Food and Drug Administration (FDA) has required that every fluoroscope measure, display, and record AK_R as well as dose-area-product (DAP) in real time. The National Electrical Manufacturers Association (NEMA) released the XR27 standard in 2013, which defines a set of minimum requirements to facilitate quality control (QC) activities on interventional fluoroscopy equipment [10]. As a function of this standard, Radiation Dose Structured Reports are generated for every fluoroscopy procedure, which documents pertinent technique

parameters such as fluoroscopy time, tube current and voltage, DAP, AK_R, and tube orientation/rotation angle for the procedure. Two examples of such dose reports are shown in Figs. 21.1 and 21.2. AK_R is not equivalent to skin dose yet still gives a useful real-time metric.

Peak skin dose (PSD) tends to be overestimated more than AK_R, as it is measured at the fixed reference point, and does not take into account the tube movement that spreads the dose into different entrance surfaces, backscatter, table transmission, patient size, or other factors. Using AK_R to estimate PSD during a procedure is, therefore, a conservative method. More accurate methods have been developed to estimate the PSD in real time [11, 12]. Newer machines have implemented improved real-time PSD estimation, utilizing collection of geometry and other exposure parameters for determining which parts of the patient graphic skin surface are exposed [13, 14]. Methods of calculating effective dose (ED) for estimation of stochastic risk based on reported DAP and tube angulation have also been investigated [15, 16].

```
Patient Info:
Name:                                          Sex:          ID:
-------------------------------------------------------------------------------------
Patient Position: HFP                                                 11-Oct-19 13:21:37
1    3D          FIXED    6sDCT Body                        6s  60F/S  11-Oct-19 14:19:18
A  90kV  240mA   3.5ms  0.0CL large 0.0Cu 48cm  1659.7µGym² 69.7mGy  82LAO   0CRA 396F

2    3D          FIXED    6sDCT Body                        6s  60F/S  11-Oct-19 14:28:38
A  90kV  326mA   3.5ms  0.1CL large 0.0Cu 48cm  2144.5µGym² 90.1mGy  82LAO   0CRA 396F

3    DR          FIXED    Single                        ***** Single  11-Oct-19 14:35:46
A  70kV  366mA  24.6ms  0.1CL small 0.0Cu 48cm   16.66µGym²  0.8mGy 180RAO   3CRA   1F

4    DR          FIXED    Single                        ***** Single  11-Oct-19 14:36:47
A  70kV  387mA  29.2ms  0.1CL small 0.0Cu 48cm   20.94µGym²  1.1mGy 180RAO   3CRA   1F

5    DR          FIXED    Single                        ***** Single  11-Oct-19 14:40:11
A  77kV  414mA  77.0ms  0.1CL small 0.0Cu 32cm   38.55µGym²  3.8mGy  80LAO   8CAU   1F

6    DR          FIXED    Single                        ***** Single  11-Oct-19 14:40:31
A  73kV  413mA  77.2ms  0.1CL small 0.0Cu 32cm   34.03µGym²  3.3mGy  00LAO  13CRA   1F

7    DR          FIXED    Single                        ***** Single  11-Oct-19 15:02:41
A  72kV  417mA  76.5ms  0.1CL small 0.0Cu 32cm   33.21µGym²  3.3mGy  83LAO  14CRA   1F

-------------------------------------------------------------------------------------

34   DR          FIXED    Single                        ***** Single  11-Oct-19 16:17:11
A  70kV  409mA  40.5ms  0.7CL small 0.0Cu 32cm   11.95µGym²  1.6mGy 178LAO   7CAU   1F

35   DR          FIXED    Single                        ***** Single  11-Oct-19 16:17:31
A  70kV  391mA  65.8ms  0.7CL small 0.0Cu 32cm   18.55µGym²  2.5mGy 174LAO   3CAU   1F


***Accumulated exposure data***                                       11-Oct-19 16:19:57
Performing Physician:                                  Exposures: 35
Total Fluoro:  35.5min                                 Total:  16354µGym²      1489mGy
A     Fluoro:  35.5min    9267.6µGym²       1139mGy    Total:  16354µGym²      1489mGy

=====================================================================================
```

Fig. 21.1 An example of a Radiation Dose Structured Report for a vertebroplasty procedure; 2 cone beam CT scans and 35 fluoroscopic runs were performed. The tube current (mA), exposure time, tube kilo-voltage, acquisition mode, and tube orientation are recorded for each CT and acquisition. The reported time for the entire procedure is 35.5 min. The procedure delivered dose-area-product (DAP) of 9267.6 µGycm^2 and AK of 1139 mGy, and 35 acquisitions delivered a DAP of 16354 µGycm^2 and AK of 1489 mGy

Report status:	Complete
Cumulative fluoroscopy time:	16.1 min
Cumulative DAP (fluoroscopy):	115109 mGycm²
Cumulative DAP (exposure):	3774 mGycm²
Total DAP:	118883 mGycm²
Cumulative Air Kerma:	894.05 mGy
Total number of acquired runs:	7
Total number of acquired images:	7
Total number of acquired exposure images:	7

Run no.	No. of images	Procedure	Speed fr/sec	kV	mA mAs	ms	DAP [mGycm²]	AK [mGy]	Rotation	Angulation	SID [cm]
1	1	Abdomen 3 fps	3	80	15		291	0.89	LAO22	0	119
2	1	Abdomen 3 fps	3	80	95		1791	5.62	RAO68	CRAN2	119
3	1	Abdomen 3 fps	3	80	22		220	1.29	LAO17	CRAN7	119
4	1	Abdomen 3 fps	3	80	33		339	1.95	LAO17	CRAN10	119
5	1	Spinal Single Shot	1	85	60		513	4.19	RAO77	CRAN1	119
6	1	Spinal Single Shot	1	85	59		447	4.16	LAO14	CAUD17	119
7	1	Spinal Single Shot	1	85	23		172	1.60	LAO14	CAUD12	119

Skin dose by Area

Cumulative Air Kerma Threshold per body area = 2000mGy

Fig. 21.2 An example of a Radiation Dose Structured Report for a vertebroplasty procedure from a different vendor. Seven fluoroscopy runs were performed where two different acquisition modes were incorporated. The reported time for the entire procedure is 16.1 min with a dose-area-product of 115109 μGycm2 for fluoroscopy and 3704 μGycm2 for 7 acquisitions. The total AK is 894.05 mGy at the reference point. This scanner also provided the AK distribution on different body parts

Hoang et al. [17] performed a retrospective review of dose parameters documented for 14 conventional fluoroscopy lumbar spine epidural steroid injections (ESI) procedures. They used the imaging techniques similar to the clinical cohort to perform the procedures on a commercially available anthropomorphic male phantom with MOSFET detectors to obtain skin and absorbed organ doses. Their mean conventional fluoroscopy time for ESI was 37 sec, and the measured skin dose is 32 mGy. Calculated ED for fluoroscopy was 0.85 mSv. Maino et al. [18] obtained dose estimation based on the dose reports of procedures performed between July 2009 and October 2016. The procedures included transforaminal epidural steroid injections (TFESI), nerve roots, and facet joint blocks. The median estimated ED was 0.19 mSv per injection per site. A retrospective study with a much larger cohort was performed by Cohen et al. [19]. Their study included an analysis of 6234 spinal injections with refinement into nine various proce-

dures performed between January and December 2012. They used a nonparametric method (bootstrap) to calculate confidence intervals of dose per injection and time per injection. They proposed preliminary reference levels of cumulative radiation skin dose (in mGy) and exposure time (in seconds) per injection site, lumbar transforaminal (13 mGy, 30 s), cervical transforaminal (6 mGy, 49 s), caudal epidural (12 mGy, 23 s), cervical facet injection (3 mGy, 36 s), lumbar facet injection (9 mGy, 20 s), interlaminar (13 mGy, 39 s), lumbar radiofrequency denervation (7 mGy, 17 s), lumbar sympathetic block (21 mGy, 39 s), cervical medial branch block (2 mGy, 25 s), lumbar medial branch block (4 mGy, 12 s), and sacroiliac joint injections (18 mGy, 37 s). Dietrich et al. [20] performed a prospective study that included 449 participants who received TFESI under fluoroscopic guidance. The mean effective participant dose for TFESI was 0.24 mSv +/−0.22 and for fluoroscopy-guided lumbar facet joint injections was 0.10 mSv +/− 0.11. These studies consistently revealed that fluoroscopy-guided spine injections are safe with low risks both deterministically (skin dose <0.05 Gy) and stochastically (effective body dose << 1 mSv).

For fluoroscopy-guided vertebroplasty or kyphoplasty, patient dose is much higher and varies much more widely. A study by Perisinakis et al. [21] showed that mean total fluoroscopy time for kyphoplasty was 10.1 minutes +/− 2.2. Mean ED for patients from kyphoplasty was 8.5–12.7 mSv, and mean gonadal dose was 0.04–16.4 mGy. A biplanar fluoroscopy study by Boszczyk et al. [22] estimated that entrance skin dose (ESD) was on an average 0.32 Gy in the anterior-posterior plane and 0.68 Gy in the lateral plane. Effective dose (cumulative from both planes) averaged 4.28 mSv. A more recent study by Li et al. [23] compared dose during vertebroplasty using single vs. two-plan fluoroscopic technique. Mean radiation dose to each patient and operator were monitored and compared between groups. The mean radiation dose to the patient was 1.97 ± 1.20 mSv (95% CI, 0.71 to 3.23) for the single-plan fluoroscopic technique group vs. 0.95 ± 0.34 mSv (95% CI, 0.85 to 1.23) for the two-plan fluoroscopic technique group. These studies showed much higher and more variable patient doses than in the category of spine injection procedures.

Extremely high radiation doses are seen in spine embolization procedures [24], which calls for attention to more severe deterministic risk as well as stochastic effects.

CT Spinal Intervention Procedures and Patient Doses

Computed tomography-guided interventional procedures were introduced shortly after CT technology emerged in the medical community [25]. With the advent of multidetector CT (MDCT), enabling fast volume scanning speed and lowered radiation dose, interventional CT-guided procedures are now performed for a wide range of diagnostic and therapeutic tasks [1, 26–35]. Major advantages of CT-guided interventional procedures include high contrast, high spatial resolution, and fast procedure time. CT is capable of providing cross-sectional and tomographic 3D images, which allows for accurate visualization of targeted anatomy as well as precise monitoring of the positioning of needles, catheters, and other devices. The choice of CT over conventional fluoroscopically guided procedures varies from institution to institution, depending on the radiologist's preferences, experience, radiation dose considerations, and equipment availability. The current generation of MDCT scanners allows multiple sub-millimeter images acquired simultaneously over a greater length. This increased speed, coupled with new image reconstruction algorithms, allows for significant dose reduction compared with traditional CT, thus enabling further increased utilization in CT spine intervention procedures. Common procedures include therapeutic injections with steroids to relieve back pain (epidural injection, nerve root block, and facet block), bone biopsy for spinal lesions, drainage of spinal fluid collections, and spinal taps [1, 26, 36, 37].

Imaging Procedures

A CT-guided procedure typically is performed in three steps: (1) A scout view to identify the anatomic region, (2) a pre-interventional planning scan to identify the targeted organ, and (3) multiple axial image acquisitions at the targeted location to track and verify the needle/catheter passage. Helical scans are employed for pre-interventional planning. These provide axial, coronal, and sagittal views of detailed anatomy. The physician uses these images to determine the location and angulation for needle insertion. The third step involves one of the following scan modes: continuous CT fluoroscopy, intermittent CT fluoroscopy, or the combination of both. Continuous CT fluoroscopy (CTF) is a real-time mode analogous to conventional fluoroscopy. The patient table is fixed in a location, while scanning is trigged by the operator stepping on a foot pedal in the room. The frame rate typically ranges from 8 to 10 fps. Alternatively, the operator employs intermittent CTF, which acquires discrete axial images at a lower frame rate and much reduced doses [29]. Intermittent CTF is similar to conventional axial scans. It has been adopted as the standard CT interventional mode by most institutions. Multiple cross-sectional images are acquired simultaneously at the rate of 1 to 2 fps and can be stopped at any moment during the procedure as determined by the physician. The total number of frames depends on the procedure scan time. The multi-slice mode provides superior volume coverage to better facilitate the position of the needle accurately. Whether using real-time or intermittent CTF, the physician remains in the CT room during image acquisition while inserting the needle/catheter. The advancement of the needle/catheter is visually tracked through displayed images on the monitor inside the room.

Patient Doses

For CT-guided spine interventional procedures, the majority of radiation dose contributions come from the pre-procedure planning scan and the CTF scan. The dose attributed from scout imaging with one or two views (anteroposterior (AP) or posteroanterior (PA)) accounts for less than 5% of the total dose. The pre-procedure planning helical scan contributes most to the total radiation dose. The planning CT scan does not require diagnostic image quality; therefore, it is typically performed with a lower dose as long as sufficient anatomic details are delineated for interventional purposes. The CTF dose varies widely, depending on whether real-time CTF or intermittent CTF is employed, as well as the duration of the actual procedure. The dose contribution from intermittent CTF as compared with the planning scan ranges from 10% to 50% [38, 39].

There are a number of published studies assessing the potential risk to patients associated with CT-guided spinal interventions. Several retrospective studies used CT dose reporting (mandatory in the majority of institutions since 1996) to assess the deterministic (skin dose) and stochastic risks (ED). The CT dose-index volume (CTDIvol) and the dose-length product (DLP) are two parameters that are documented in CT reports after the procedure is performed. An example of such a report is shown in Fig. 21.3. Leng et al.

Dose							
#	Scan label	Scan mode	mAs	kV	CTDIvol [mGy]	DLP [mGy*cm]	Phantom type [cm]
1	SCOUT	Surview		120	0.085	3	BODY 32 CM
2	AX SOURCE	Helical	53	120	3.3	61.7	BODY 32 CM
3		Station...	30	120	2.4×7	16.8	BODY 32 CM

Fig. 21.3 An example of a CT dose report for an epidural spinal injection procedure. The CTD dose-index volume (CTDIvol) and dose-length product (DLP) are listed for scout view, the pre-procedure planning helical scan, and the intermittent (stationary) CT fluoroscopy sequence. The helical scan gives the highest DLP

surveyed the mean skin dose and ED of 571 patients who underwent CT-guided interventional procedures, including spinal procedures, during the period of March to July 2008. The mean skin dose and ED for each procedure were calculated. The mean skin doses varied significantly among different procedures, but all were below 2 mGy (the minimum dose threshold for transient [non-permanent] skin effects). The mean ED also varied significantly across procedure types. For spinal bone biopsy procedures, ED ranged from 9 to 25 mSv [38]. Joemai et al. [40] reviewed 210 CT-guided interventional procedures including vertebroplasties, spine biopsies, and diskography, among many others. While most procedures resulted in ED in the range of 0–20 mSv, vertebroplasties had much higher dose, greater than 100 mSv. Yang et al. [41] collected dictation reports and radiation dose data from 9,143 consecutive CT-guided interventional procedures in adult patients from 2012 to 2017. The size-specific dose estimates for bone biopsy ranged from 13 mSv to 26 mSv. In an effort to reduce the radiation dose, Greffier et al. [42] demonstrated that procedures including spinal or peri-spinal infiltration, vertebral expansion, and bone biopsies could be performed with ED ranging from 1.9 mSv to 11.5 mSv. A study by Guberina et al. [43] found ED ranging from 4.5 to 8.5 mSv associated with CT spinal procedures. Lazarus et al. [44] reviewed 994 studies, including 585 ESIs, 228 nerve root blocks, and 90 facet blocks, performed over a 12-month period in 2012. For all studies, procedure time averaged 7:34 ± 5:05 sec, and DLP averaged 75 ± 61 mGy·cm. This translated to ED of 1 mSv (±0.8). Hoang et al. [17] performed a similar study in 42 CTF procedures for ESIs and estimated that the average dose was 0.45 mSv. Dietrich et al. [20] performed a prospective study on TFESIs and facet joint injections under fluoroscopic or CT guidance between October 2009 and April 2016. The mean ED for CT procedures was 0.33 mSv. These studies clearly indicate that epidural injections are associated with very low patient dose, under 1 mSv. Dose varies greatly by procedure; bone biopsy varies typically from 10 to 30 mSv, while vertebroplasties may potentially be much higher.

Dose Comparison: Fluoroscopy-Guided vs. CT-Guided Procedures

It is commonly acknowledged that the fluoroscopic procedure is typically associated with less radiation exposure than CT procedures. The skin-entrance dose rate for fluoroscopy is on an average less than 1 mGy per min, while in CT, it is greater than 1 mGy per second. This is one of the primary reasons that fluoroscopy has remained the top modality choice for image-guided procedures, in particular for complex and lengthy procedures.

In Hoang et al.'s study [17], the calculated ED for fluoroscopically guided ESI was 0.85 mSv, compared with 0.45 mSv for CTF. The greatest contribution to the radiation dose from CTF-guided ESI came from the planning lumbar spine CT scan, which had an ED of 2.90 mSv when z-axis ranged from L2 to S1. This resulted in a total ED for CTF-guided ESI of 3.35 mSv, or about 4 times greater than similar fluoroscopically guided procedures. Maino et al.'s study [18] showed a greater difference with 8 times the dose increase with CTF. A study with more recent CT technology, however, showed that the difference was much smaller (~ 35%) in TFESI procedures, where the CT-guided procedures also had much tighter dose ranges among different patients [20].

Doses to Procedure Practitioners

Radiation exposure to physicians, nurses, and technologists arises primarily due to radiation scattered from the patient. Similar to patient dose, there is also a wide distribution of occupational dose in image-guided interventional procedures.

The two categories of people affected by the radiation doses are patients and staff in a diagnostic radiology procedure setting. The amount of energy deposited in the tissue of patients can largely lead to stochastic effects. The workers typically get occupational dose which is orders of magnitude lower than that of the patient during a single procedure, but this may become significant for a worker who performs large numbers of pro-

cedures, especially if shielding and other ALARA precautions, as mentioned above, are not observed.

Occupational Dose in Fluoroscopy-Guided Procedures

Botwin et al. [45] evaluated radiation exposure to spinal interventionists while performing TFESIs. The average exposure per procedure (over 100 total) was 0.7 mrem to extremities, 0.4 mrem to the lens of the eye, and 0.3 mrem to the whole-body dosimeter worn outside the lead apron. No radiation was detectable at the inside of the apron. Compared with the International Commission on Radiological Protection (ICRP) threshold limits [46], these doses pose very low risk to physicians performing TFESLs. Theocharopoulos et al. [47] investigated different surgical procedures (hip, spine, kyphoplasty, and vertebroplasty) and estimated their relative contribution to the surgeon's effective radiation dose. The study used a mobile C-arm fluoroscopy unit on an anthropomorphic phantom, employing protocols commonly used in image-guided orthopedic surgery. The study concluded that the surgeon's ED attributed from kyphoplasty and vertebroplasty is the highest among all spine procedures. They found an ED of 9.6 mrem per procedure for kyphoplasty and vertebroplasty while wearing an apron, thyroid protection, and leaded goggles. They further suggested that the there is a non-negligible increased lifetime risk for cancer development for surgeons who performed kyphoplasty and vertebroplasty regularly.

Occupational Dose in CT-Guided Procedures

Typically, physicians and staff remain outside the scanner room during the scout and pre-procedural CT planning; exposure to scattered radiation only occurs during the CTF phase. Several studies have assessed physician doses related to CT spine injections. Joemai et al. [40] monitored radiologists, nurses, and technologists with electronic dosimeters during 547 CT interventional procedures. The derived median occupational ED was 0.3 mrem/procedure for the interventional radiologists and 0.04 mrem/procedure for the assisting radiologists and radiology technologists. These doses are quite low relative to the annual occupational limit.

In general, the physician's dose is proportional to patient's dose. A study by Dietrich et al. [20], however, has shown that radiation exposure in fluoroscopy-guided lumbar spinal injections was lower for participants and higher for physicians when compared with CT-guided injections. There are no published data of occupational dose for more complex CT spine procedures. The reason is perhaps that such procedures are not routinely performed due to the concern with potentially high patient doses.

Dose Reduction in Fluoroscopy-Guided and CT-Guided Procedures

Radiation exposure by imaging-guided intervention is not negligible; "as low as reasonably achievable" (ALARA) represents a practice mandate to reduce doses to both patients and practitioners. Practitioners have the responsibility for lowering patient dose under the guidance of ALARA. The major objective for dose reduction in interventional procures is threefold: (1) to follow ALARA principles, (2) to use the least possible dose of radiation required, and (3) to obtain a detailed high-quality image.

The ALARA methods that need to be used to minimize patient dose are size, distance, and time, i.e., collimate to the treatment size of the X-ray field, increase the distance from the focal spot of the X-ray tube to the skin or image receptor, and reduce the exposure time. These main techniques have been detailed in a 10-step approach by the International Atomic Energy Agency (IAEA) [48]. It is important to note that patient dose reduction techniques apply equally well to reduction in occupational exposure to staff, as the amount of scattered radiation from the patient is directly proportional to patient dose,

although typically at levels between 0.01% and 0.1% of that received by the patient.

For fluoroscopy-guided procedures, general techniques include maximizing the distance from the radiation source to patient, minimizing the distance from the detector to patient, collimating the X-ray beam to the area of interest, lowering the frame rate to the minimum acceptable level, reducing beam settings [current (mA)/kilovoltage (kVp)], using C-arm rotation to spread the entrance skin dose, and limiting the number of radiographic acquisitions [49]. In modern fluoroscopy systems, the beam setting and dose rates are dictated by the vendor's algorithm of AEC (automatic exposure control). The modification of AEC can be a joint effort between practitioners and manufacturers. Recent technology developments have led to drastic exposure reduction, which is potentially applicable to many different procedures. For example, recent developments in methods of image noise reduction have also enabled more than 50% exposure and dose reduction, without compromising the image quality [50, 51].

The most effective step to reduce patient exposure is to maximize the source-to-surface distance (SSD), that is, the distance between the X-ray tube and the patient. Radiation dose is inversely proportional to the square of the distance from the source; for example, moving the patient dose entrance location from 45 cm to 38 cm increases the entrance dose by over 40%. It is, therefore, imperative to maximize this distance. In an effort to curb this effect, the FDA has limited SSD to a minimum of 38 cm for stationary units and 30 cm for mobile and portable units. Additionally, tube output is limited to 10 R/min for normal fluoroscopy mode and 20 R/min for high-output (or "boost") mode, which is to be used sparingly. At an SSD of 38 cm, typical exposure rates are ~1–2 R/min for a thin body, 3–5 R/min for an average body, and 8–10 R/min for heavy patients.

While patient positioning with respect to the X-ray source is important, positioning relative to the image receptor is also crucial. Unless otherwise required, the image receptor should always be positioned as close as possible to the patient. Elevation of the image receptor increases geometric magnification, which in turn drives up tube output via AEC. Additionally, a smaller distance between the patient and detector allows for a greater capture of scattered radiation; exposure to staff with large patient to detector distances can be significantly increased. Proper collimation is an equally effective technique. Reduction of field size to the clinical interest not only reduces patient and staff dose but also reduces scatter and improves image contrast.

Intimate knowledge of machine parameters and controls specific to each vendor and system (e.g., GE, Philips, Siemens, Toshiba, etc.) is essential. Different dose mode selections may be available such as low dose (reduced patient dose, increased image noise), high dose (increased patient dose, reduced image noise), low frame rate (reduced patient dose and reduced frame rate), and others. When image quality allows, use of low dose mode and/or a lower frame rate is encouraged. High dose rate mode may be needed for large patients or for seeing greater detail but should not be routinely used.

Exposure to the same area of the patient skin should be avoided if possible; this may be accomplished by using different projections and rotating the beam entrance port around the patient. Larger patients or thicker body parts increase beam attenuation, which increases exposure via AEC. Similarly, lateral and oblique exposures can increase the entrance surface dose. Field size and patient habitus play a significant role in the amount of rotation; on average, an angulation of 22–26 degrees (minimum) is required to have any appreciable effect on radiation dose [52].

With older fluoroscopic units utilizing image intensifier (II) detection technology, physical magnification (or "mag" mode) can significantly increase doses. For example, decreasing the field of view by a factor of two increases the dose rate by a factor of four; switching from 12" (32 cm) to 9" (22 cm) will increase the relative patient entrance dose rate by over 200%. Newer technology flat-panel detectors do not present this effect, as magnification occurs digitally/electronically.

Minimization of the number of CINE "runs," digital acquisitions, and DSA acquisitions will

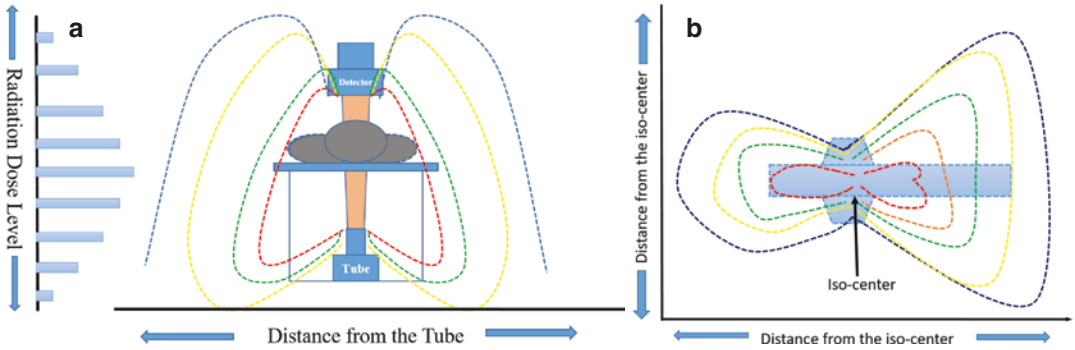

Fig. 21.4 The isodose decreases as distance from the patient increases. (**a**) Fluoroscopy system used for interventional procedures is generally configured with the X-ray tube positioned beneath the patient table and the X-ray detector (either a flat-panel detector or an image intensifier) positioned above the patient table. The radiation to staff during the procedure results from scatters originating from the patient. The backscattered radiation from the entrance side of the patient (i.e., the tube side) is much greater than forward-scatter radiation at the exiting side of patient. (**b**) For CT, the gantry blocks the scatter intensity. The scattered intensity, therefore, has a dumbbell distribution on both sides of the gantry. Scatter intensity decreases as distance increases from the isocenter, where the X-ray enters the patient

reduce exposure, as these techniques use a high radiation dose rate to obtain a series of high-resolution images with reduced image noise. Thus, the radiation dose per frame for digital and CINE acquisitions can be 15 times greater than for fluoroscopy. The number and length of these acquisitions may be the greatest source of patient radiation dose in interventional radiology procedures.

Practitioners have an advantage over patients in the availability of dose reduction techniques, as they are able to wear protective lead garments. Since staff stay at the bedside during interventional procedures, it is imperative for them to wear lead aprons, thyroid shields, and leaded eye protection during procedures and to include leaded gloves during procedures where the hands may enter the primary field. These garments have demonstrated more than 90% radiation protection to whole body and more than 50% to hands [47, 53]. In a study by Paulson, dosimeters were placed on the radiologist's collar (outside the thyroid shield) and fingers during 57 spinal injections and 17 spinal biopsies. This study found that the estimated whole-body dose was 1.7 times higher per procedure for physicians not wearing a lead apron [29]. During CT fluoroscopy phases, practitioners should step to the side of the gantry to avoid scatted radiation when able (Fig. 21.4). Maximizing distance from the patient also reduces exposure to the operator. For fluoroscopy, measurements have shown that scattered radiation from a patient's body is more intense at the entrance side of X-ray beam. Therefore, it is better to stand on the side of the detector, that is, the exit side, and not on the X-ray tube side during a fluoroscopic procedure (see Fig. 21.4).

For CT-guided procedures, all the general dose reduction techniques employed in conventional CT are applicable. The helical planning scan delivers most of the total dose and should therefore be strictly limited to the spinal segment of interest and performed with the lowest acceptable image quality. Dose modulation should always be employed. In analogy to AEC used in fluoroscopy, CT dose reference level (Quality Reference mAs, Dose Right Index [DRI], and Image Noise Index) should be adjusted to the minimal level acceptable to the physician's need. Iterative reconstruction [54, 55] has generally replaced the traditional filtered back projection as the standard CT image reconstruction. Iterative methods have significantly reduced the image noises on the reconstructed images, especially

those acquired with low-dose CT techniques. The combination of dose modulation and iterative reconstruction has shown significant dose reduction in CT spine imaging [56, 57]. Employing intermittent CTF is also important to reduce the total dose of CT-guided procedures. This is analogous to lowered pulse rate in fluoroscopy.

Radiation Biology and Radiation Effects

Ionizing radiation on an electromagnetic spectrum is that which carries enough energy to detach electrons from atoms or molecules, thereby ionizing them (Fig. 21.5) [58]. This ionization can affect chemical bonds within molecules, which in turn affects the cells and tissues, eventually affecting the organs and finally affecting the whole body. This level of damage can happen at dose and dose rates relevant to diagnostic radiology. There is a wide range in the amount of radiation doses delivered by various diagnostic procedures (Table 21.1) of which typically the highest numbers come from a CT scan of the abdomen and pelvis with contrast (~20 mSv) [59–62].

Radiation Injury to the DNA

Deoxyribonucleic acid (DNA) contains the genetic information of the cell. DNA is a large molecule that has a characteristic double-helix structure consisting of two strands, each made up of a sequence of nucleotides. The backbone of the DNA strand is made of alternating sugar and

Table 21.1 Representative effective radiation doses delivered by various diagnostic procedures [59–62]

Examination	Effective dose, mSv
Conventional radiology	
Lumbar spine	0.5–1.8
Chest	0.007–0.05
Computed tomography (CT)	
Head	0.9–4.0
Chest	4–18
Abdomen	3.5–25
Pelvis	3–10
Cervical spine	~3
Lumbar spine	~ 6
Interventional cardiology	
Coronary angiography	2–16
Ablation procedures	6.6–59
Percutaneous coronary intervention	7–57
Cardiac catheterization and stent placement	7–15

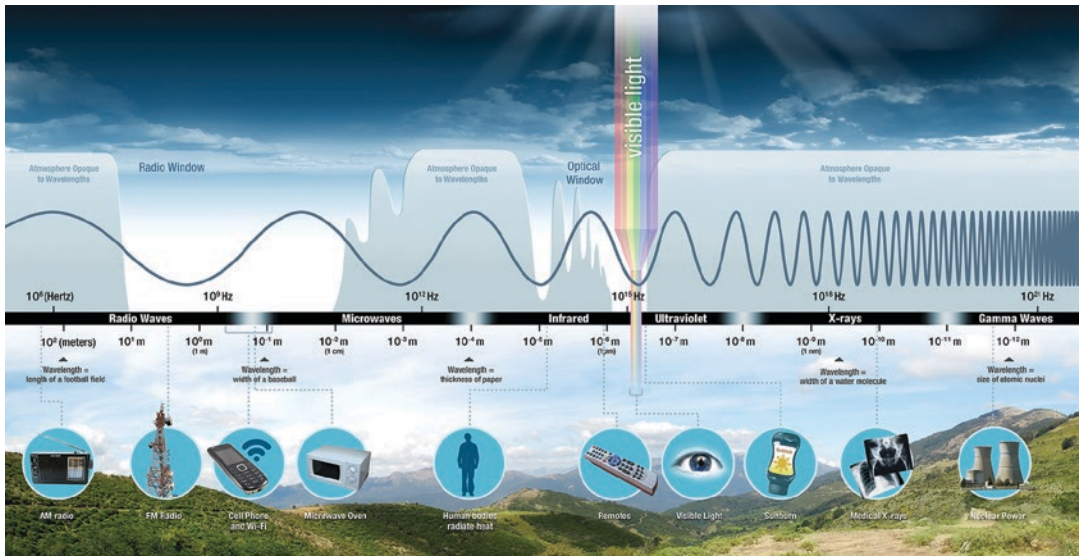

Fig. 21.5 The electromagnetic spectrum (NASA, public domain, via Wikimedia Commons). https://commons.wikimedia.org/wiki/File:Electromagnetic_spectrum,_NASA_illustration.jpg

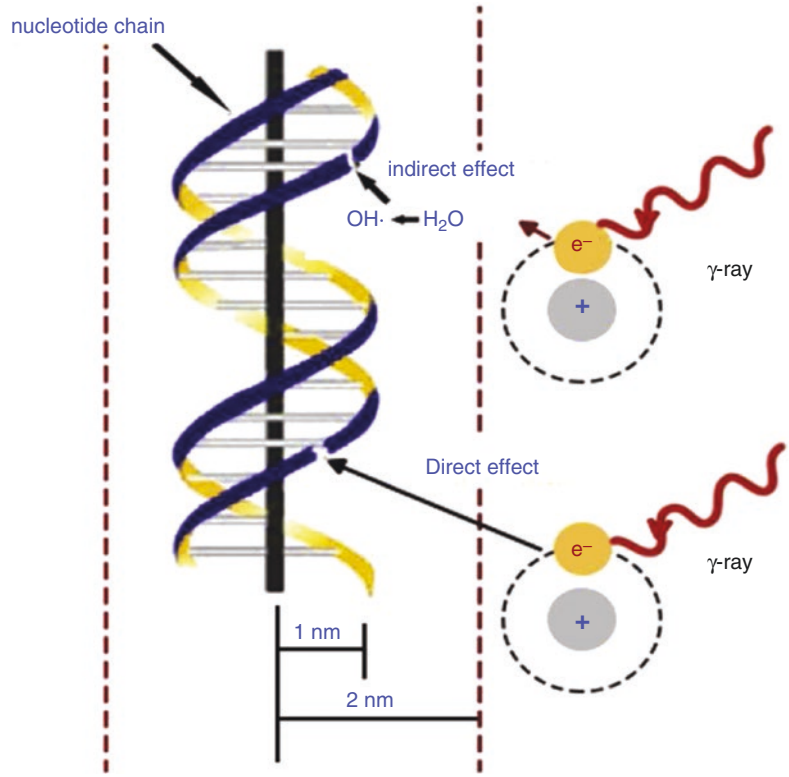

Fig. 21.6 Cell damage caused by direct or indirect ionization radiation. (From Desouky et al. [63], with permission Elsevier)

phosphate groups. A nucleotide is a subunit of DNA and is composed of a "base" linked to a sugar (deoxyribose) attached to a phosphate group. Any damage to DNA can be lethal. Radiation damage to the cell can be caused by two mechanisms: direct action (ionization) and indirect action (ionization) of radiation on the DNA molecules (Fig. 21.6) [63].

Direct Effect of Ionizing Radiation

In the direct action, the radiation interacts with the DNA molecule directly, disrupting the molecular structure. This can lead to cell damage or even cell death. The damaged cells that survive may later induce carcinogenesis or other abnormalities. The process is known as direct because the interaction occurs directly between a particle and a cellular component without an intermediary step. This type of DNA damage becomes predominant with high-LET radiations such as α-particles and neutrons and high radiation doses [64–67].

Linear energy transfer (LET) is the amount of energy that an ionizing particle transfers to the material traversed per unit distance measured in eV/cm. LET is used to quantify the effects of ionizing radiation on biological specimens. LET largely determines the "biological effectiveness." High LET ionizing radiation particles can deposit a large amount of energy in a small distance and are more damaging. Examples of high LET radiation particles are neutrons, protons, and alpha particles. The DNA damage caused by high LET radiations is more difficult to repair than low LET radiations doses.

Indirect Effect of Ionizing Radiation

In the indirect action, the radiation interacts with water molecules near to sensitive targets. This presents a much larger probability of occurrence than direct action, as water is the major constituent of the cell and other organic molecules in the cell. During this impact, energy gets absorbed by the water molecule leading to formation of ion

pairs and reactive oxygen metabolites such as free hydroxyl radicals (OH). In turn, these free radicals interact with cellular atoms and molecules damaging cellular proteins and may form additional free radicals [64–67].

The number of free radicals produced by ionizing radiation will depend on the total absorbed dose. Indirect effects of damage are typically observed with low LET radiation particles such as photon radiation (X-rays and gamma rays, electrons, beta rays). About two-thirds of the biological damage caused by low LET radiations (sparsely ionizing radiation) is due to indirect action. This is more common to what occurs in a diagnostic radiology procedure setting.

DNA damage is the primary cause of cell death caused by diagnostic radiation. Radiation exposure produces a wide range of lesions in DNA such as single-strand breaks (SSBs), double-strand breaks (DSBs), base damage, protein-DNA cross links, and protein-protein cross links. The numbers of lesions induced in the DNA of a cell by a dose of 1–2 Gy is approximately >1000 base damages, ~1000 SSBs, and ~40 DSBs. DNA repair mechanisms are important for the recovery of cells from radiation, but unrepaired or mis-repaired damage to DNA will lead the exposed cell to mutation or chromosome damage. Cell mutations might further lead to cancer or hereditary effects. Chromosomal damage, when severe, can often lead to cell death.

Radiation damage to mammalian cells can be divided into three categories: (1) lethal damage (LD), which is irreversible and irreparable and, by definition, leads to cell death; (2) potentially lethal damage (PLD), the component of radiation damage that can be modified by post irradiation environmental conditions; and (3) sublethal damage (SLD), which under normal circumstances can be repaired in hours unless additional SLD is added (e.g., from a second dose of radiation). Additional SLD can accumulate to form LD. SLD repair is manifested by the increase in survival observed if a dose of radiation is split into two fractions separated by a time interval.

The law of Bergonie and Tribondeau states that the radiosensitivity of a biological tissue is directly proportional to the mitotic activity and inversely proportional to the degree of differentiation of its cells. ICRP Publications 60 and 103 [46, 68] list tissue-weighting factors (w_T) that help assign a particular organ or tissue the proportion of the stochastic effects resulting from irradiation of the tissue compared to a uniform whole-body radiation. The cell cycle has two well-defined time periods: mitosis (M), where division takes place, and the period of DNA-synthesis (S-phase). The S and M portions of the cell cycle are separated by two periods (gaps) G1 and G2. Replication of the genome occurs in the S-phase, and mitotic propagation to daughter generations occurs in the G2/M phases. Radiosensitivity differs throughout the cell cycle: late S-phase is the most radio resistant, G2/M being most radiosensitive and the G1 phase taking an intermediate position.

Radiation doses in the order of several Sieverts may lead to cell loss. Cells are generally regarded as "killed" by radiation if they have lost reproductive integrity, even if they physically survived. Loss of reproductive integrity can occur by apoptosis, necrosis, mitotic catastrophe, or induced senescence. Apoptosis or programmed cell death can typically occur naturally or result from insult to the cell environment. Cellular necrosis generally occurs after high radiation doses.

Biological effects of ionizing radiation in humans can occur either in irradiated individuals (somatic effects) that can lead to *deterministic effects* and *stochastic effects* or in descendants (hereditary/genetic effects) leading to *stochastic effects*. Deterministic effects typically have a minimum threshold and severity of the effect related to dose. Stochastic effects, on the other hand, are usually described by the linear-non-threshold (LNT) model and are related to excess cancer induction.

Deterministic Effects

These effects describe a cause-and-effect relationship between radiation and radiation-induced side effects. Deterministic effects have a threshold below which the effect does not occur (Fig. 21.7). Deterministic effects may occur a few hours or days after exposure (i.e., early skin reaction) or may require months or years before

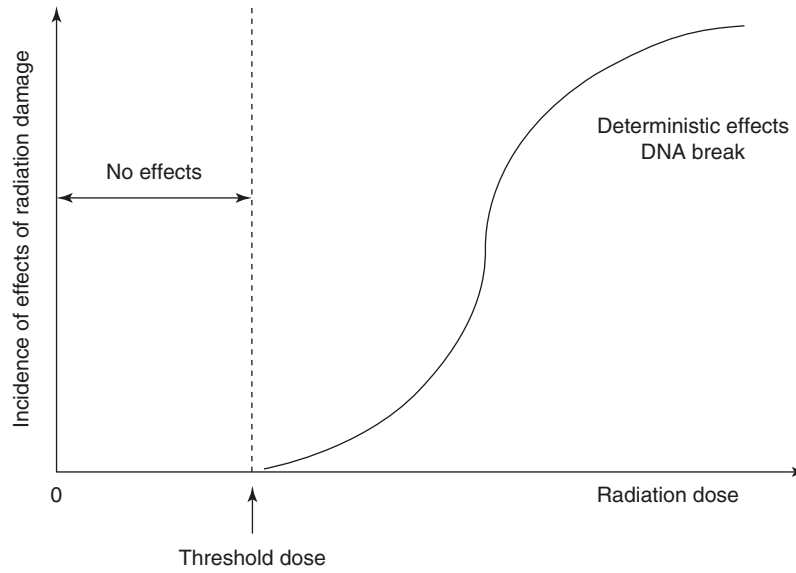

Fig. 21.7 Deterministic effects. Responses that increase in severity with increased dose. If the dose increases, the severity of an effect increases. All early effects and most tissue late effects are a deterministic effect

expression (i.e., cataract of the eye lens) [69–71]. Threshold doses in tissues and organs in adults exposed to acute, fractionated, or protracted and chronic radiation exposure can be found in Bushberg and Boone [58].

Effects of radiation on normal tissues are based largely on functional and histopathological endpoints. Therefore, radiation injury to tissues can also be classified according to the time after exposure for clinical symptoms to manifest: acute (early response within a few weeks) and late effects (response that is shown after many months or years).

Acute Effects

Acute responses occur primarily in tissues with rapid cell renewal, where cell division is required to maintain the function of the organ. Examples of early responding tissues where acute effects are seen are in the bone marrow, gastrointestinal tract, and skin. An exposure of approximately 2 Gy (200 rads) dose can manifest itself with hematopoietic syndrome, including pancytopenia, infection, and hemorrhage [72]. An intermediate-level exposure to dose of >6 Gy (600 rads) can present itself with gastrointestinal (GI) syndrome—dehydration, electrolyte abnormalities, GI bleeding, and fulminant enterocolitis [72]. This can happen within hours of exposure. A high dose exposure to >20 to 30 Gy (2000 to 3000 rads) can cause cardiovascular and central nervous system syndrome with refractory hypotension and circulatory collapse [72]. GI syndrome and the neurovascular syndrome are irreversible.

Late Effects

Late responses tend to occur under normal conditions in organs whose parenchymal cells divide rarely or infrequently, such as the liver or kidney and central nervous system or muscle, respectively. Late responses can also occur in tissues that manifest early reactions, such as the skin/subcutaneous tissue and intestine; however, the nature of these reactions (subcutaneous fibrosis, intestinal stenosis) is quite different from the early reactions. A common late reaction is the slow development of tissue fibrosis and vascular damage that occurs in many tissues and is often seen in cancer patients a number of years after radiation treatment.

Typical tissue reactions to diagnostic level of radiation doses are seen in the skin, lens of the eye, and reproductive fertility in males and females.

Radiation-Induced Skin Reaction

A wide variety of expressions of radiation-induced skin effects have been reported based on exposure levels. Early transient erythema, similar

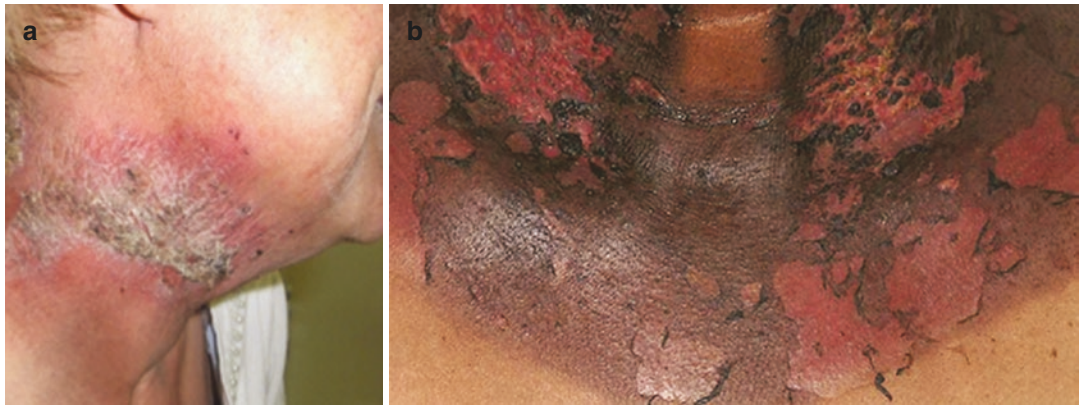

Fig. 21.8 Radiation-induced skin reactions: (**a**) radiation dermatitis with moderate erythema and scaly dry desquamation and (**b**) acute radiation dermatitis with confluent moist desquamation. (From Hymes et al. [77], with permission Elsevier)

to sunburn, is the most common visual symptom and occurs within a few hours after irradiation. A second and more severe erythema can develop after a latent period of 8–10 days due to an inflammatory reaction of the skin. This is bright red in color, limited to the radiation field, and accompanied by a sensation of heat and itching. Radiation-induced skin reactions can be divided based upon the dose exposed: transient erythema in the human skin occurs after single doses greater than 2 Gy; general erythema occurs at doses greater than about 7 Gy; and moist desquamation and ulceration occur after doses of 15 to 20 Gy (Fig. 21.8) [73–77].

Radiation-Induced Cataract Formation

The lens of the eye contains transparent lens fibers and a small number of dividing cells within the lens capsule. If dividing epithelium is injured by radiation, opacity of the lens (cataracts) will develop. There is no mechanism for removal of injured cells and abnormal fibers. The frequency of cataract formation varies with exposure to chronic doses vs. acute doses. The time period between exposure and the appearance of cataract varies between 6 months and 30 years. The radiation dose greatly influences the latent period. In general, the higher the dose, the shorter the latent period. Moderate doses of radiation can produce cataracts in a few individuals, with the incidence increasing to 100% in individuals exposed to a single dose of 2 Gy or higher to the lens of the eye [78, 79].

Stochastic Effects

These are effects that occur by chance and consist primarily of cancer and genetic effects. As the dose to an individual increases, the probability that cancer or a genetic effect will occur also increases. For probabilistic effects, the probability of the occurrence of an effect is a function of dose, but the severity of a stochastic effect is not a function of dose (Fig. 21.9). Stochastic effects are assumed to exhibit no threshold dose below which they cannot occur [80]. The major stochastic effects of concern at typical diagnostic radiology levels are cancers and genetic effects. They are exclusively late effects because they do not appear until years after radiation exposures. Other examples of stochastic effects of radiation are leukemia and hereditary effects. Stochastic radiation effects typically have a latent period. Leukemia has a minimum latency of about 2 years after exposure; the pattern of risk over time peaks after 10 years (most cases occur in the first 15 years) and decreases thereafter (Fig. 21.10) [81]. Solid tumors show a longer latency than leukemia, by anything from 10 to 60 years or even more.

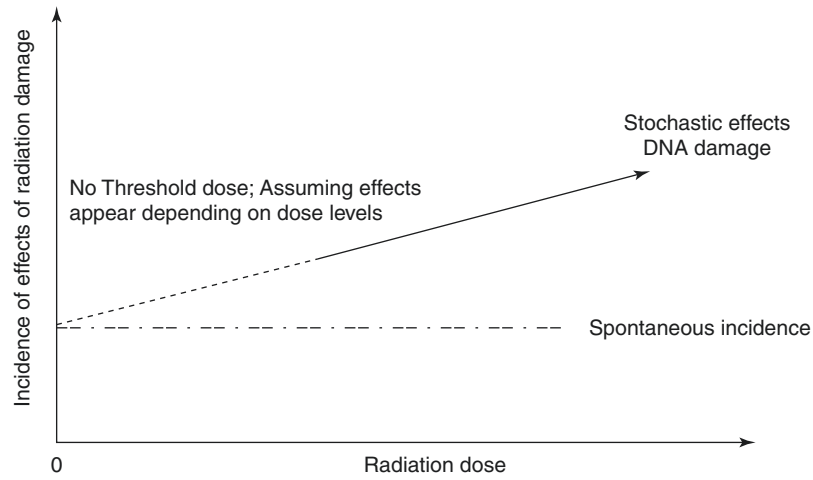

Fig. 21.9 Stochastic radiation effects that occur by chance, generally occurring without a threshold level of dose, whose probability is proportional to the dose and whose severity is independent of the dose

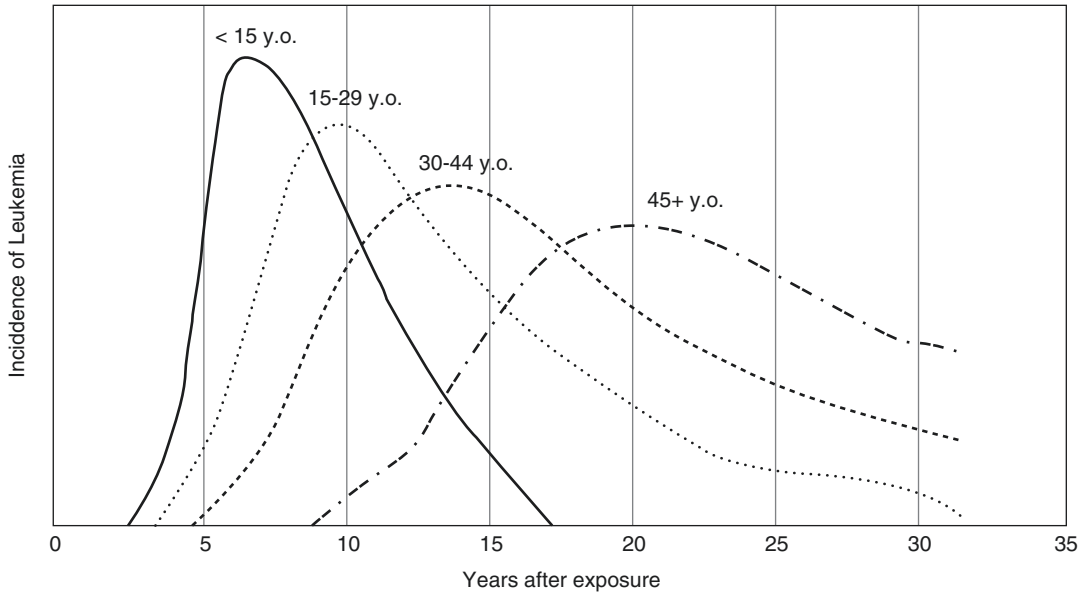

Fig. 21.10 Stochastic radiation effects related to the time course and latency period. Effect of age at the time of exposure on the incidence of leukemia (all forms except chronic lymphocytic leukemia) among the atomic bomb survivors [81]

Radiation Safety Regulations and Requirements

As with all imaging modalities utilizing ionizing radiation, radiation exposure limits and radiation safety requirements are vital to provide a safe working environment for physicians and staff, patients, and members of the public. Unlike radioactive material regulations, which are generally implemented at the federal or national level, regulations and requirements specific to machine-produced ionizing radiation (e.g., CT, fluoroscopy) are typically realized at the state and/or local level. While specific requirements

will vary with local governance, central concepts are broadly similar across all locations. Some important differences for practices outside of the United States are detailed at the end of this section.

Occupational Radiation Safety Requirements and Regulatory Basis

Regulatory requirements, especially occupational exposure limits to clinical employees, are based on an imperfect understanding of chronic effects of low-level exposure to ionizing radiation. High-level exposures and corresponding effects, both deterministic and stochastic, are relatively well-known with good statistical correlation. At lower levels of exposure, statistical correlation to stochastic effects with high confidence is lacking. Based on the available data and guidance from scientific bodies (such as the ICRP, the National Research Council, etc.), regulatory agencies have unanimously incorporated the LNT model to describe radiation risk.

The LNT model (Fig. 21.11) indicates that any radiation exposure results in an increased risk of stochastic effects, usually stated as excess cancer induction. Inherent in this model is the assumption that there is no threshold dose for stochastic effects and that stochastic risk increases linearly with radiation dose [82, 83]. This in turn precipitates what is known as the "as low as reasonably achievable," or ALARA, concept, as described above. The ALARA paradigm is used as a cost-benefit type analysis; some exposure to radiation is inevitable but should be managed and minimized to the extent that is practical. The ALARA concept follows the principles of justification, optimization, and limitation. Justification ensures that the exposure and any correlating risks are justified from a cost-benefit standpoint. Optimization relates to the application of dose reduction techniques and methods, such as shielding for staff or protocol and equipment adjustments for patients. Limitation is the application of hard limits of radiation exposure below which, in the worst case, risks are considered acceptable [46].

It is worth noting that the LNT model and ALARA principle have been in place for decades; however, over the last 10–20 years, the increased use of medical imaging and data collection capabilities have led to models with smaller confidence intervals in the low dose region and even some models that suggest health benefits at low doses [84–86]. Nevertheless, other recent studies have supported the LNT model [19]. While far from being decisive, the bulk of available data appears to be trending toward a flatter slope at lower doses in the

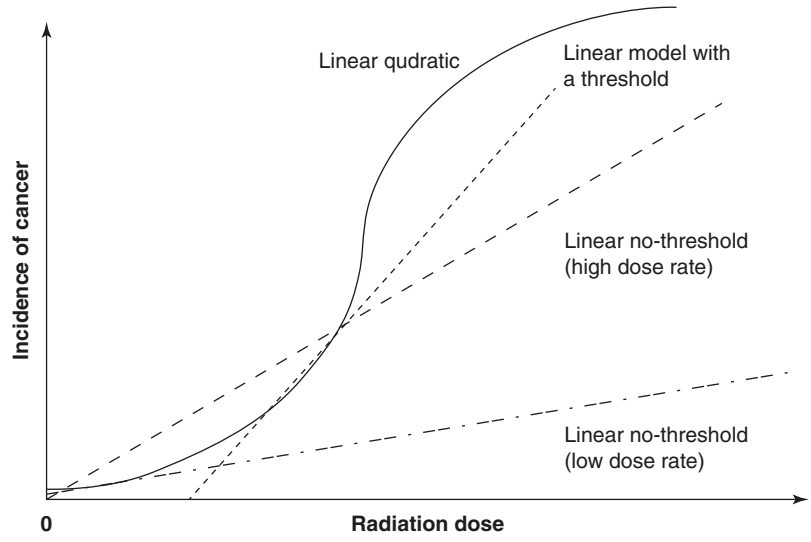

Fig. 21.11 The linear-non-threshold (LNT) model. Dose-response model used in radiation protection to estimate the stochastic health effects on the human body due to exposure to ionizing radiation [82]

0–50 mSv range. This indicates that stochastic risks are likely less pronounced at lower doses. Be that as it may, regulatory bodies have shown hesitation to deviate from the LNT model for several reasons, most importantly being that the data are not yet conclusive and that the LNT model is conservative in its estimates of risk [87].

In the United States, annual radiation whole-body exposure limits are set such that the risk of excess cancer induction is less than 1% for solid tumors and less than 0.1% for leukemia [82]. In addition to annual whole-body exposure limits, annual limits are set for exposures to the extremities, individual organs, and lens of the eye. Many states also incorporate limits of annual exposure to occupied minors, pregnant workers, and members of the public. The Nuclear Regulatory Commission (NRC), which maintains regulatory oversight of the use of radioactive material, has instituted annual exposure limits, which have generally been adopted at the state level regarding machine-produced radiation. Additionally, the Conference of Radiation Control Program Directors (CRCPD), a professional organization that provides guidance to state- and local-level regulators, has urged the acceptance of NRC limits for machine-produced radiation. Nevertheless, some states still adhere to other or outdated limits, such as those mandated by the Occupational Safety and Health Administration. A summary of these limits is given in Table 21.2 [88–91].

Regulatory bodies maintain occupational radiation dose limits on an annual or quarterly basis, which follows from a cumulative (or absolute) model of stochastic radiation risk. This model assumes that the stochastic effects from subsequent radiation exposures are additive. This is true for multiple exposures over relatively short time frames, in terms of biological repair processes (i.e., hours to days) [87, 92]. However, the LNT model implies, and epidemiological data support, that stochastic radiation risk follows a relative risk model when applied over large time frames [93]. Stated simply, the nth exposure to the same anatomical area carries the same radiation risk as the first exposure (given similar doses). This applies to low-level exposures to both patients and staff.

Table 21.2 Occupational dose limits for the United States and Europe [88–91]. The limits vary depending on the affected part of the body

US Nuclear Regulatory Commission (NRC) and Conference of Radiation Control Program Directors Limits (CRCPD) limits		
Exposed organ or tissue	Dose limit (mSv)	Time period
Whole body	50	Annually
Individual organ	500	
Skin or extremity	500	
Lens of the eye	150	
Fetus	5	
Minors (whole body)	5	
Occupational Safety and Health Administration (OSHA) limits		
Whole body	12.5	Quarterly (50 mSv annual equivalent)
Head and trunk		
Active blood-forming organs		
Lens of the eye		
Gonads		
Extremity	187.5	Quarterly (750 mSv annual equivalent)
Skin of whole body	75	Quarterly (300 mSv annual equivalent)
European limits		
Whole body	20	Annually
	50	In a single year for special circumstances; 5-year moving average must not exceed 20 mSv
Individual organ	N/A	N/A
Skin or extremity	500	Annually
Lens of the eye	20	Annually
	100	Total over 5 consecutive years; 5-year moving average must not exceed 50 mSv
Fetus	1	Annually
Minors (whole body)	6	Annually

Adapted from: Title 10 Code of Federal Regulations (10CFR Part20), Part 20 "Standards for Protection against Radiation," and European Agency for Safety and Health 2015. The limits vary depending on the affected part of the body

International Regulations

Practitioners operating outside of the United States must adhere to radiation regulations in their country of practice and should look to

their local regulatory body. In many instances, countries follow standards similar to the United States; in general, recommendations by international scientific bodies, such as the International Atomic Energy Agency (IAEA) and ICRP, align closely with domestic regulations. An important exception applies to member countries of the European Union (EU) and those that have adopted EU guidance. The EU Directive 2013/59/Euratom "Protection Against Ionizing Radiation" provides requirements with significantly lower annual occupational limits, as shown in Table 21.2 [89, 91]. For many physicians, radiation protection methods must be aggressively applied to maintain these limits, especially with regard to exposure to the lens of the eye.

Radiation Safety Requirements for Facilities and the Public

In addition to regulatory requirements for occupationally exposed individuals, annual exposure limits are mandated for members of the public. Members of the public include patients when they are not being exposed to radiation as part of an exam, visitors, hospital vendors and service personnel, and clinical staff whose regular duties do not involve exposure to ionizing radiation (e.g., clerical and janitorial staff, etc.). Unlike occupationally exposed "radiation workers," it is assumed that the public has not been educated on the risks of radiation exposure and are therefore unable to make a risk-benefit analysis in accordance with the ALARA concept. Concordantly, public exposures are limited to low levels, with stochastic risks of excess cancer induction due to radiation at less than 0.1% [46]. Limits are typically set at 1 mSv per year, not to exceed 20 μSv in any 1 hour. Outside of radiology and interventional areas, these limits are easy to achieve in clinical facilities. However, in and around areas where ionizing radiation is utilized, access controls and facility shielding may be required to maintain these limits. These are discussed in depth in the next section.

Radiation Safety Requirements for Patients

Patient radiation exposures are not mandated or regulated at the government level. Medical need and appropriateness of the exam dictate whether a patient receives ionizing radiation, and cost-benefit analyses are inherently weighed during selection of the exam and consenting. However, ALARA concepts apply, and techniques should be chosen to minimize patient dose while maintaining adequate image quality.

Extended or multiple interventional procedures may result in excessive patient skin or organ dose that significantly exceeds occupational limits. While stochastic risks that manifest many years later are important to consider, short-term deterministic effects, such as erythema and epilation, have more immediate clinical relevance.

Skin entrance doses of greater than 2 Gy can result in transient erythema and epilation, although for most patients, this becomes more likely in the 4–5 Gy range [24]. These dose levels are common for interventional radiology and interventional cardiology procedures, although less so for interventional spine and pain procedures [94]. For patients requiring multiple visits, cumulative dose over a fairly short time period (<6 months) can build to levels in the 15 Gy or greater range, which requires proactive follow-up over the following 18–24 months to treat skin effects such as dry and moist desquamation, necrosis, ulceration, etc. Because of these possibilities, the Joint Commission has instituted a Sentinel Event classification for cases resulting in over 15 Gy of skin dose to the same area within 6 months [95]. A Sentinel Event is defined as a patient safety event (not primarily related to the natural course of the patient's illness or underlying condition) that reaches a patient and results in death, permanent harm, or severe temporary harm. This is not an exposure limit but rather a checkpoint for caregivers; further exposures to ionizing radiation above this point should only be considered in order to prevent morbidity and mortality. Patient exposures above these levels

may necessitate a root cause analysis or notification in order to comply with accreditation standards.

In an effort to minimize the number of Sentinel Events, the Joint Commission (and many State regulatory agencies) have instituted fluoroscopy dose notification requirements. Facilities are required to set dose threshold (or reference) levels that prompt further review and/or patient evaluation. For example, patient cumulative doses in a single procedure >1 Gy has to be reported to the Radiation Safety Committee. Exposures exceeding 3 Gy may prompt a notification to the patient with instructions to self-evaluate and care for possible mild erythema; exposures exceeding, say, 10 Gy may prompt further instructions and a follow-up visit, as well as a notification to the interventionist to justify any further exposures that may lead to Sentinel Event levels. It is important to note that these actions and levels are flexible and must be enacted at each facility as appropriate. All doses must be entered into the patient's medical record. Patients who are likely to have deterministic injury need to be followed. The physician or the interventionist must have fluoroscopy privileges. Accurate skin dose estimates require extended calculations, accounting for many variables such as table transmission factors, backscatter factors, C-arm rotation angles, etc. [11, 12, 52]. In many institutions, practical reference levels may be set at certain thresholds for air kerma, DAP, or fluoroscopy time to facilitate real-time notifications within the clinic [94, 96]. The Joint Commission added a Sentinel Event category for radiation overdose involving prolonged fluoroscopy with a cumulative dose of more than 15 Gy to a single field in January 2019. All fluoroscopy machines manufactured after June 2006 must measure and display a reference patient radiation dose.

Annual Equipment Evaluation

The ACR requires that the performance of all fluoroscopic and CT equipment be evaluated upon installation to ensure compliance with manufacturer specifications and regulations regarding maximum exposures and proper functioning. These evaluations must be performed by a qualified medical physicist (QMP) or a clinical engineer approved by the respective state laws. These evaluations are repeated periodically to ensure consistency over time and must be performed annually at a minimum. The ultimate goal of these quality control tests is to establish and maintain performance standards that will result in diagnostic or interventional studies with the appropriate diagnostic image quality at the lowest reasonable radiation dose. Similar evaluations are performed after major repairs that could impact imaging performance of the equipment or the radiation output (e.g., X-ray tube replacement, filter change, detector change).

The complete list of parameters that are evaluated as part of the annual fluoroscopic equipment evaluation is listed in Table 21.3 [97]. As appropriate to intended use of the unit, these tests will be performed for both automated exposure controls and manual techniques. The designations of

Table 21.3 Fluoroscopic equipment evaluation tests to be performed by a qualified medical physicist annually [97]

1. Visual equipment checklists
2. Integrity of unit assembly
3. Operation of alerts and interlocks
4. Other radiation safety functions
5. Appropriateness of protocols (fluoroscopic and acquisition)
6. Pediatric protocols and equipment configurations
7. Isocenter location
8. Radiation field size measurement
9. Acquisition display monitor(s) performance
10. Collimation and radiation beam alignment
11. Tube potential (kVp) accuracy and reproducibility
12. Minimum beam quality (half-value layer)
13. Automatic dose rate control performance
14. Image quality: system high contrast resolution
15. Image quality: system low contrast sensitivity
16. Displayed radiation metrics accuracy
17. Image receptor air kerma rate
18. Patient entrance air kerma rate for a "typical" adult patient and a "typical" pediatric patient if applicable
19. Maximum patient entrance air kerma rate
20. Image receptor performance
21. Image artifacts
22. PACS adequacy

these tests to be done at Acceptance Testing, Performance Evaluation, or periodic QC are listed in the American College of Radiology-American Association of Physicists in Medicine (ACR-AAPM) Technical Standard for Diagnostic Medical Physics Performance Monitoring of Fluoroscopic Equipment [97].

A regular audit of patient dose indices is also performed by comparing the facility's CT and fluoroscopy dose information with national benchmarks such as the ACR Dose Index Registry. Patient radiation dose rates with the imaging technical parameters (kVp, mAs) for each protocol are collected at least annually and reported to the radiology managers. Additionally, most states require annually evaluated technical parameters (kVp, mAs, and dose rate) to be reported on a card that is placed on the machine. The results obtained each year are compared against the previous year to identify any potential equipment failures. Deviations of more than 10% require assessment by clinical engineering, with follow-up reevaluation by the QMP. Detailed physicist reports of these compliance tests and any findings are reported to management and maintained for regulatory and accreditation inspections for at least 3 years.

Apart from annual machine evaluations, the QMP will also assist the facility in understanding and developing policies and procedures to evaluate risks to patients, personnel, and physicians from studies and interventions requiring prolonged radiation exposure [49]. The QMP will also assist the Radiation Safety Officer in evaluating the radiation risks to occupationally exposed individuals and members of the public who may be affected by the fluoroscopy or CT equipment.

Conclusion

This chapter has summarized the uses of fluoroscopy and CT protocols for spinal treatments, with special emphasis on radiation exposure and protection principles. The various biological effects that can occur based on these radiation exposures have also been summarized, including models related to cancer risk. Various protection strategies that can help protect from radiation injuries for patients and staff have also been provided. The ultimate goal is to deliver the minimum amount of radiation dose to patients necessary to acquire good-quality images for diagnostic and interventional treatments. Reduction of radiation dose to the patient correlates directly to reduction of radiation dose to the operators and staff.

References

1. Manchikanti L, Pampati V, Falco FJ, Hirsch JA. Growth of spinal interventional pain management techniques: analysis of utilization trends and Medicare expenditures 2000 to 2008. Spine. 2013;38(2):157–68.
2. Miller DC, Patel J. Smith CC; Spine Intervention Society's Patient Safety Committee. Fact finders for patient safety: radiation safety for interventional spine procedures. Pain Med. 2018;19(3):629–30.
3. Bundy JJ, Chick JFB, Hage AN, Gemmete JJ, Srinivasa RN, Johnson EJ, et al. Contemporary interventional radiology dosimetry: analysis of 4,784 discrete procedures at a single institution. J Am Coll Radiol. 2018;15(9):1214–21.
4. Balaguru D, Rodriguez M, Leon S, Wagner LK, Beasley CW, Sultzer A, Numan MT. Comparison of skin dose measurement using nanoDot® dosimeter and machine readings of radiation dose during cardiac catheterization in children. Ann Pediatr Cardiol. 2018;11(1):12–6.
5. Meyer P, Regal R, Jung M, Siffert P, Mertz L, Constantinesco A. Feasibility of a semiconductor dosimeter to monitor skin dose in interventional radiology. Med Phys. 2001;28(10):2002–6.
6. Glennie D, Connolly BL, Gordon C. Entrance skin dose measured with MOSFETs in children undergoing interventional radiology procedures. Pediatr Radiol. 2008;38(11):1180–7.
7. Giordano BD, Baumhauer JF, Morgan TL, Rechtine GR. Cervical spine imaging using standard C-arm fluoroscopy: patient and surgeon exposure to ionizing radiation. Spine (Phila Pa 1976). 2008;33(18):1970–6.
8. Giordano C, D'Ercole L, Gobbi R, Bocchiola M, Passerini F. Coronary angiography and percutaneous transluminal coronary angioplasty procedures: evaluation of patients' maximum skin dose using Gafchromic films and a comparison of local levels with reference levels proposed in the literature. Phys Med. 2010;26(4):224–32.
9. International Electrotechnical Commission. Medical electrical equipment, Part 2–43. Particular requirements for the safety of X-ray equipment for interventional procedures. IEC 60601–2-43; 2000.

10. National Electrical Manufacturers Association. NEMA XR 27. X-ray equipment for interventional procedures user quality control mode. Rosslyn: National Electrical Manufactureres Association. 1 Jan 2013.
11. Jones AK, Pasciak AS. Calculating the peak skin dose resulting from fluoroscopically guided interventions. Part I: methods. J Appl Clin Med Phys. 2011;12(4):231–44.
12. Jones AK, Pasciak AS. Calculating the peak skin dose resulting from fluoroscopically-guided interventions. Part II: case studies. J Appl Clin Med Phys. 2012;13(1):174–86.
13. Johnson PB, Borrego D, Balter S, Johnson K, Siragusa D, Bolch WE. Skin dose mapping for fluoroscopically guided interventions. Med Phys. 2011;38(10):5490–9.
14. Rana V, Rudin S, Bednarek D. A tracking system to calculate patient skin dose in real-time during neurointerventional procedures using a biplane X-ray imaging system. Med Phys. 2016;43(9):5131–44.
15. Compagnone G, Giampalma E, Domenichelli S, Renzulli M, Golfieri R. Calculation of conversion factors for effective dose for various interventional radiology procedures. Med Phys. 2012;39(5):2491–8.
16. Le Heron JC. Estimation of effective dose to the patient during medical X-ray examinations from measurements of the dose-area product. Phys Med Biol. 1992;37(11):2117–26.
17. Hoang JK, Yoshizumi TT, Toncheva G, Gray L, Gafton AR, Huh BK, et al. Radiation dose exposure for lumbar spine epidural steroid injections: a comparison of conventional fluoroscopy data and CT fluoroscopy techniques. AJR Am J Roentgenol. 2011;197(4):778–82.
18. Maino P, Presilla S, Colli Franzone PA, van Kuijk SM, Perez RS, Koetsier E. Radiation dose exposure for lumbar transforaminal epidural steroid injections and facet joint blocks under CT vs. fluoroscopic guidance. Pain Pract. 2018;18(6):798–804.
19. Cohen S, Liu A, Gurvitz M, Guo L, Therrien J, Laprise C, et al. Exposure to low-dose ionizing radiation from cardiac procedures and malignancy risk in adults with congenital heart disease. Circulation. 2018;137(13):1334–45.
20. Dietrich TJ, Peterson CK, Zeimpekis KG, Bensler S, Sutter R, Pfirrmann CW. Fluoroscopy-guided versus CT-guided lumbar steroid injections: comparison of radiation exposure and outcomes. Radiology. 2019;290(3):752–9.
21. Perisinakis K, Damilakis J, Theocharopoulos N, Papadokostakis G, Hadjipavlou A, Gourtsoyiannis N. Patient exposure and associated radiation risks from fluoroscopically guided vertebroplasty or kyphoplasty. Radiology. 2004;232(3):701–7.
22. Boszczyk BM, Bierschneider M, Panzer S, Panzer W, Harstall R, Schmid K, et al. Fluoroscopic radiation exposure of the kyphoplasty patient. Eur Spine J. 2006;15(3):347–55.
23. Li YY, Huang TJ, Cheng CC, Wu MH, Lee CY. Comparing radiation exposure during percutaneous vertebroplasty using one- vs. two-fluoroscopic technique. BMC Musculoskelet Disord. 2013;14:38.
24. Miller DL, Balter S, Noonan PT, Georgia JD. Minimizing radiation-induced skin injury in interventional radiology procedures. Radiology. 2002;225(2):329–36.
25. Alfidi RJ, Haaga J, Meaney TF, MacIntyre WJ, Gonzalez L, Tarar R, et al. Computed tomography of the thorax and abdomen; a preliminary report. Radiology. 1975;117(2):257–64.
26. Gangi A, Dietemann J-L, Mortazavi R, Pfleger D, Kauff C, Roy C. CT-guided interventional procedures for pain management in the lumbosacral spine. Radiographics. 1998;18(3):621–33.
27. Daly B, Templeton PA. Real-time CT fluoroscopy: evolution of an interventional tool. Radiology. 1999;211(2):309–15.
28. Silverman SG, Tuncali K, Adams DF, Nawfel RD, Zou KH, Judy PF. CT fluoroscopy-guided abdominal interventions: techniques, results, and radiation exposure. Radiology. 1999;212(3):673–81.
29. Paulson EK, Sheafor DH, Enterline DS, McAdams HP, Yoshizumi TT. CT fluoroscopy-guided interventional procedures: techniques and radiation dose to radiologists. Radiology. 2001;220(1):161–7.
30. Carlson SK, Bender CE, Classic KL, Zink FE, Quam JP, Ward EM, et al. Benefits and safety of CT fluoroscopy in interventional radiologic procedures. Radiology. 2001;219(2):515–20.
31. Froelich JJ, Ishaque N, Regn J, Saar B, Walthers EM, Klose KJ. Guidance of percutaneous pulmonary biopsies with real-time CT fluoroscopy. Eur J Radiol. 2002;42(1):74–9.
32. Heyer CM, Brus LJ, Peters SA, Lemburg SP. Efficacy of CT-guided biopsies of the spine in patients with spondylitis–an analysis of 164 procedures. Eur J Radiol. 2012;81(3):e244–e9.
33. Trumm CG, Pahl A, Helmberger TK, Jakobs TF, Zech CJ, Stahl R, et al. CT fluoroscopy-guided percutaneous vertebroplasty in spinal malignancy: technical results, PMMA leakages, and complications in 202 patients. Skelet Radiol. 2012;41(11):1391–400.
34. Gupta AC, Yoo AJ, Stone J, Barr JC, Brook A, Tutton S, et al. Percutaneous sacroplasty. J Neurointerv Surg. 2012;4(5):385–9.
35. Kim GR, Hur J, Lee SM, Lee HJ, Hong YJ, Nam JE, et al. CT fluoroscopy-guided lung biopsy versus conventional CT-guided lung biopsy: a prospective controlled study to assess radiation doses and diagnostic performance. Eur Radiol. 2011;21(2):232–9.
36. Gold MM, Miller TS, Farinhas JM, Altschul DJ, Bello JA, Brook AL. Computed tomography–guided lumbar drain placement. J Neurosurg Spine. 2008;9(4):372–3.
37. Toomayan GA, Major NM. Utility of CT-guided biopsy of suspicious skeletal lesions in patients with known primary malignancies. AJR Am J Roentgenol. 2011;196(2):416–23.
38. Leng S, Atwell TD, Yu L, Mandrekar J, Lewis BD, Woodrum DA, McCollough CH. Radiation dose

reduction for CT-guided renal tumor cryoablation. AJR Am J Roentgenol. 2011;196(5):W586–91.
39. Kloeckner R, dos Santos DP, Schneider J, Kara L, Dueber C, Pitton MB. Radiation exposure in CT-guided interventions. Eur J Radiol. 2013;82(12):2253–7.
40. Joemai RM, Zweers D, Obermann WR, Geleijns J. Assessment of patient and occupational dose in established and new applications of MDCT fluoroscopy. AJR Am J Roentgenol. 2009;192(4):881–6.
41. Yang K, Ganguli S, DeLorenzo MC, Zheng H, Li X, Liu B. Procedure-specific CT dose and utilization factors for CT-guided interventional procedures. Radiology. 2018;289(1):150–7.
42. Greffier J, Pereira FR, Viala P, Macri F, Beregi JP, Larbi A. Interventional spine procedures under CT guidance: how to reduce patient radiation dose without compromising the successful outcome of the procedure? Phys Med. 2017;35:88–96.
43. Guberina N, Forsting M, Ringelstein A, Suntharalingam S, Nassenstein K, Theysohn J, et al. Radiation exposure during CT-guided biopsies: recent CT machines provide markedly lower doses. Eur Radiol. 2018;28(9):3929–35.
44. Lazarus MS, Forman RB, Brook AL, Miller TS. Radiation dose and procedure time for 994 CT-guided spine pain control procedures. Pain Physician. 2017;20(4):E585–E91.
45. Botwin KP, Thomas S, Gruber RD, Torres FM, Bouchlas CC, Rittenberg JJ, et al. Radiation exposure of the spinal interventionalist performing fluoroscopically guided lumbar transforaminal epidural steroid injections. Arch Phys Med Rehabil. 2002;83(5):697–701.
46. The 2007 Recommendations of the International Commission on Radiological Protection. ICRP publication 103. Ann ICRP. 2007;37(2–4):1–332.
47. Theocharopoulos N, Perisinakis K, Damilakis J, Papadokostakis G, Hadjipavlou A, Gourtsoyiannis N. Occupational exposure from common fluoroscopic projections used in orthopaedic surgery. J Bone Joint Surg Am. 2003;85(9):1698–703.
48. International Atomic Energy Agency. Patient dose optimization in fluoroscopically guided interventional procedures: final report of a coordinated research project. IAEA-TECDOC-1641. Vienna, Austria: International Atomic Energy Agency; 2010.
49. Mahesh M. National Council on radiation protection and measurements. NCRP 168: its significance to fluoroscopically guided interventional procedures. J Am Coll Radiol. 2013;10(7):551–2.
50. Söderman M, Holmin S, Andersson T, Palmgren C, Babić D, Hoornaert B. Image noise reduction algorithm for digital subtraction angiography: clinical results. Radiology. 2013;269(2):553–60.
51. Dekker LR, van der Voort PH, Simmers TA, Verbeek XA, Bullens RW, van't Veer M, et al. New image processing and noise reduction technology allows reduction of radiation exposure in complex electrophysiologic interventions while maintaining optimal image quality: a randomized clinical trial. Heart Rhythm. 2013;10(11):1678–82.
52. Pasciak AS, Jones AK. Does "spreading" skin dose by rotating the C-arm during an intervention work? J Vasc Interven Radiol. 2011;22(4):443–52.
53. Synowitz M, Kiwit J. Surgeon's radiation exposure during percutaneous vertebroplasty. J Neurosurg Spine. 2006;4(2):106–9.
54. Willemink MJ, de Jong PA, Leiner T, de Heer LM, Nievelstein RA, Budde RP, et al. Iterative reconstruction techniques for computed tomography part 1: technical principles. Eur Radiol. 2013;23(6):1623–31.
55. Willemink MJ, Leiner T, de Jong PA, de Heer LM, Nievelstein RA, Schilham AM, et al. Iterative reconstruction techniques for computed tomography part 2: initial results in dose reduction and image quality. Eur Radiol. 2013;23(6):1632–42.
56. Swanson JO, Alessio AM, White KK, Krengel WF, Friedman SD, Vining NC, et al. Spine computed tomography radiation dose reduction. Spine. 2015;40(20):1613–9.
57. Gervaise A, Teixeira P, Villani N, Lecocq S, Louis M, Blum A. Dose optimization and reduction in musculoskeletal CT including the spine. In: Tack D, Kalra M, Gevenois P, editors. Radiation dose from multidetector CT. Berlin, Heidelberg: Springer; 2012. p. 369–87.
58. Bushberg JT, Seibert JA, Leidholdt EM Jr, Boone JM. The essential physics of medical imaging. 3rd ed. Philadelphia: Lippincott Williams & Wilkins.Wolters Kluwer; 2012.
59. Ait-Ali L, Andreassi MG, Foffa I, Spadoni I, Vano E, Picano E. Cumulative patient effective dose and acute radiation-induced chromosomal DNA damage in children with congenital heart disease. Heart. 2010;96(4):269–74.
60. Fazel R, Krumholz HM, Wang Y, Ross JS, Chen J, Ting HH, et al. Exposure to low-dose ionizing radiation from medical imaging procedures. N Engl J Med. 2009;361(9):849–57.
61. Mettler FA Jr, Huda W, Yoshizumi TT, Mahesh M. Effective doses in radiology and diagnostic nuclear medicine: a catalog. Radiology. 2008;248(1):254–63.
62. Padmanabhan D, Shankar S, Chandrashekharaiah A, Deshpande S. Strategies to reduce radiation exposure in electrophysiology and interventional cardiology. US Cardiol Rev. 2019;13(2):117–22.
63. Desouky O, Ding N, Zhou G. Targeted and non-targeted effects of ionizing radiation. J Radiat Res Appl Sci. 2015;8(2):247–54.
64. Juhl JH, Crummy AB. Paul and Juhl's essentials of radiologic imaging. Philadelphia: Lippincott; 1993.
65. White SC, Pharoah MJ. Oral radiology: principles and interpretation. 7th ed. St. Louis: Mosby/Elsevier; 2014.
66. Miles DA, Van Dis ML, Williamson GF, Jensen CW. Radiographic imaging for the dental team. 4th ed. Philadelphia: Elsevier; 2009.
67. Hall EJ, Giaccia AJ. Radiobiology for the radiologist. 6th ed. London: Lippincott Williams & Wilkins; 2006.

68. International Commission on Radiological Protection. Radiation protection. 1990 recommendations of the International Commission on Radiological Protection. ICRC 21(1–3). Oxford UK: Pergamon Press; 1991.
69. Joiner MC, Van der Kogel AJ. Basic clinical radiobiology. 4th ed. London: Edward Arnold; 2009.
70. Stewart F, Akleyev A, Hauer-Jensen M, Hendry J, Kleiman N, Macvittie T, et al. ICRP publication 118: ICRP statement on tissue reactions and early and late effects of radiation in normal tissues and organs–threshold doses for tissue reactions in a radiation protection context. Ann ICRP. 2012;41(1–2):1–322.
71. Van der Kogel AJ, Joiner MC. The dose rate effect. In: Basic clinical radiobiology. 4th ed. London: Edward Arnold; 2009. p. 158–68.
72. Clements BW, Casani JAP. Disasters and public health: planning and response. 2nd ed. Oxford UK/Cambridge MA: Butterworth-Heinemann; 2016.
73. Balter S, Hopewell JW, Miller DL, Wagner LK, Zelefsky MJ. Fluoroscopically guided interventional procedures: a review of radiation effects on patients' skin and hair. Radiology. 2010;254(2):326–41.
74. Chambers CE, Fetterly KA, Holzer R, Lin PJ, Blankenship JC, Balter S, Laskey WK. Radiation safety program for the cardiac catheterization laboratory. Catheter Cardiovasc Interv. 2011;77(4):546–56.
75. Koenig TR, Wolff D, Mettler FA, Wagner LK. Skin injuries from fluoroscopically guided procedures: part 1, characteristics of radiation injury. Am J Roentgenol. 2001;177(1):3–11.
76. Bray FN, Simmons BJ, Wolfson AH, Nouri K. Acute and chronic cutaneous reactions to ionizing radiation therapy. Dermatol Ther (Heidelb). 2016;6(2):185–206.
77. Hymes SR, Strom EA, Fife C. Radiation dermatitis: clinical presentation, pathophysiology, and treatment 2006. J Am Acad Dermatol. 2006;54(1):28–46.
78. Bitarafan Rajabi A, Noohi F, Hashemi H, Haghjoo M, Miraftab M, Yaghoobi N, et al. Ionizing radiation-induced cataract in interventional cardiology staff. Res Cardiovasc Med. 2015;4(1):e25148.
79. Loganovsky KN, Marazziti D, Fedirko PA, Kuts KV, Antypchuk KY, Perchuk IV, et al. Radiation-induced cerebro-ophthalmic effects in humans. Life (Basel). 2020;10(4):41.
80. Hamada N, Fujimichi Y. Classification of radiation effects for dose limitation purposes: history, current situation and future prospects. J Radiat Res. 2014;55(4):629–40.
81. Ishimaru T, Hoshino T, Ichimaru M, Okada H, Tomiyasu T, Tsuchimoto T, et al. Leukemia in atomic bomb survivors, Hiroshima and Nagasaki, 1 October 1950-30 September 1966. Radiat Res. 1971;45(1):216–33.
82. National Research Council. Health risks from exposure to low levels of ionizing radiation: BEIR VII phase 2. Washington, DC: The National Academies Press; 2006. https://doi.org/10.17226/11340.
83. NCRP. Report No. 136—Evaluation of the linear-nonthreshold dose-response model for ionizing radiation. Issued 4 Jun 2001. Bethesda: National Council on Radiation Protection and Measurements.
84. Rossi HH. Sensible radiation protection. Health Phys. 1996;70(3):394–5.
85. Simmons JA, Watt DE, Gooden DS. Radiation protection dosimetry: a radical reappraisal. Med Phys. 1999;26(9):2047.
86. Rithidech KN. Health benefits of exposure to low-dose radiation. Health Phys. 2016;110(3):293–5.
87. Feinendegen LE, Cuttler JM. Biological effects from low doses and dose rates of ionizing radiation: science in the service of protecting humans, a synopsis. Health Phys. 2018;114(6):623–6.
88. Conference of Radiation Control Program Directors (CRCPD). Suggested state regulations for control of radiation. Part D standards for protection against radiation. Frankfort: CRCPD, Mar 2003. https://cdn.ymaws.com/www.crcpd.org/resource/resmgr/docs/SSRCRs/dpart.pdf.
89. United States Nuclear Regulatory Commission. NRC regulations title 10, Code of federal regulations. Part 20 standards for protection against radiation, 10 CFR 20. 21 May 1991. https://www.nrc.gov/reading-rm/doc-collections/cfr/part020/full-text.html. Page Last Reviewed/Updated 29 Dec 2020. Accessed 1 Jan 2021.
90. United States Department of Labor. Occupational Safety and Health Administration. 1910.1096—Ionizing Radiation, Standard 1910.1096. https://www.osha.gov/laws-regs/regulations/standardnumber/1910/1910.1096. Accessed 1 Jan 2021.
91. Council of the European Union. Council Directive 2013/59/EURATOM laying down basic safety standards for protection against the dangers arising from exposure to ionising radiation, and repealing Directives 89/618/Euratom, 90/641/Euratom, 96/29/Euratom, 97/43/Euratom and 2003/122/Euratom. 5 Dec 2013.
92. Frankenberg-Schwager M. Induction, repair and biological relevance of radiation-induced DNA lesions in eukaryotic cells. Radiat Environ Biophys. 1990;29(4):273–92.
93. Miller DL, Balter S, Cole PE, Lu HT, Berenstein A, Albert R, et al. Radiation doses in interventional radiology procedures: the RAD-IR study part II: skin dose. J Vasc Interv Radiol. 2003;14(8):977–90.
94. Durand DJ, Dixon RL, Morin RL. Utilization strategies for cumulative dose estimates: a review and rational assessment. J Am Coll Radiol. 2012;9(7):480–5.
95. The Joint Commission. Radiation risks of diagnostic imaging and fluoroscopy. The Joint Commission Sentinel Event Alert 47. Oakbook Terrace: The Joint Commission, 24 Aug 2011. Revised Feb 2019.
96. Metaxas VI, Messaris GA, Gatzounis GD, Tzortzidis FN, Konstantinou DT, Panayiotakis GS. Institutional (local) diagnostic reference levels in fluoroscopically guided spine surgery. Eur J Radiol. 2017;90:50–9.
97. American College of Radiology/American Association Physics in Medicine. ACR-AAPM technical standard for diagnostic medical physics performance monitoring of fluoroscopic equipment. 2018 (CSC/BOC). Amended 2018. (Resolution 44) https://www.acr.org/-/media/ACR/Files/Practice-Parameters/Fluoro-Equip.pdf. Accessed 1 Jan 2021.